Single-Molecule Spectroscopy Using Nanoporous Membranes

Guillaume A. T. Chansin,[†] Rafael Mulero,[‡,||] Jongin Hong,[§,||] Min Jun Kim,[‡] Andrew J. deMello,[§] and Joshua B. Edel*,[†,§]

Institute of Biomedical Engineering, Imperial College London, South Kensington, SW7 2AZ, United Kingdom, Department of Mechanical Engineering & Mechanics, Drexel University, 3141 Chestnut Street, Philadelphia, Pennsylvania 19104, and Department of Chemistry, Imperial College London, South Kensington, SW7 2AZ, United Kingdom

ABSTRACT

We describe a novel approach for optically detecting DNA translocation events through an array of solid-state nanopores that potentially allows for ultra high-throughput, parallel detection at the single-molecule level. The approach functions by electrokinetically driving DNA strands through sub micrometer-sized holes on an aluminum/silicon nitride membrane. During the translocation process, the molecules are confined to the walls of the nanofluidic channels, allowing 100% detection efficiency. Importantly, the opaque aluminum layer acts as an optical barrier between the illuminated region and the analyte reservoir. In these conditions, high-contrast imaging of single-molecule events can be performed. To demonstrate the efficiency of the approach, a 10 pM fluorescently labeled λ-DNA solution was used as a model system to detect simultaneous translocation events using electron multiplying CCD imaging. Single-pore translocation events are also successfully detected using single-point confocal spectroscopy.

In the post-genomic era, much effort is still focused on identifying genes responsible for specific biological functions (or diseases) and determining the DNA sequence bearing the information. The need to perform such processes in a rapid and efficient manner has dictated the creation of a new generation of experimental tools. Of particular note has been the considerable progress in the development of microfluidic systems for use in the chemical and biological sciences.[1] Interest in such technology has been driven by a range of fundamental features that accompany system miniaturization. These features include the ability to process and handle small volumes of fluid, improved analytical performance when compared to macroscale analogues, reduced instrumental footprints, low unit costs, facile integration of functional components, and the exploitation of atypical fluid dynamics to control molecules in both time and space. On the basis of these beneficial characteristics, microfluidic chip devices have been used to good effect in a wide variety of applications including nucleic acid separations, protein analysis, small-molecule organic synthesis, DNA amplifica-

tion, immunoassays, DNA sequencing, cell manipulations, and medical diagnostics.[2]

More recently, significant effort has centered on scaling down microfluidic systems to create features such as channels and pores with cross-sectional dimensions most easily measured in nanometers. Such "nanofluidic" devices open up new opportunities for fundamental and applied studies of chemical and biological phenomena. In basic terms, nanofluidics describes fluid flow in and around structures with dimensions smaller than a few hundred nanometers. A number of defining characteristics separate fluid flow at the nanoscale from flow in larger environments. First, flow occurs in structures that are comparable to natural scaling lengths, e.g., the Debye length in electrolyte solutions. Second, internal surface area-to-volume ratios can be enormous. Third, diffusion becomes an extremely efficient mass transport mechanism at this scale. And finally, the ultra-small volumes associated with nanofluidic environments allow effective confinement of analyte molecules to defined regions and thus theoretically allow perfect detection efficiencies in analytical applications. All of these characteristics can be exploited to significant advantage when processing or analyzing chemical and biological systems. For example, single-molecule-based fragment-sizing methods have previously been demonstrated in devices involving small capillaries and flow cytometry.[3] Moreover, single-molecule DNA
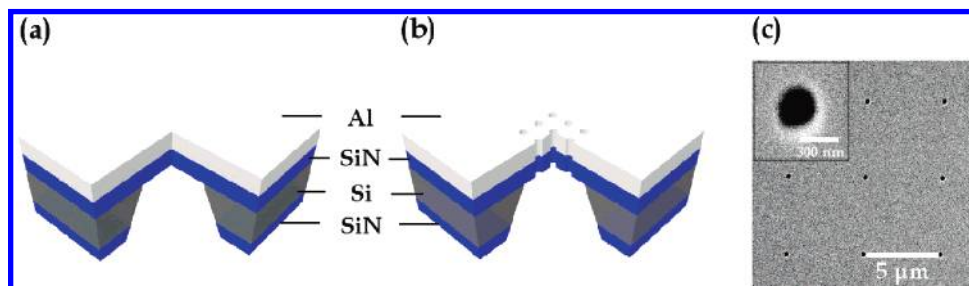
---

* Corresponding author. E-mail: joshua.edel@imperial.ac.uk.
† Institute of Biomedical Engineering, Imperial College London.
‡ Department of Mechanical Engineering & Mechanics, Drexel University.
§ Department of Chemistry, Imperial College London.
|| These authors contributed equally towards this publication.

Figure 1. Schematic of device fabrication: (a) a free-standing 200 nm thick silicon nitride membrane is fabricated using standard photolithographic techniques and KOH wet etching followed by aluminum deposition; (b) milling of submicrometer holes by focused ion beam; (c) SEM image of nanopore array. The top left inset shows a higher resolution SEM image of a single pore.

fragment sizing has also been demonstrated in microchannel environments.[4] In these situations, channel dimensions are still relatively large, and thus restrictions are imposed on the optimal resolution that can be obtained, achievable analytical throughput, and nonperfect molecular detection efficiencies. For example, large channel dimensions require relatively large observation windows for uniform illumination of the entire channel width. Therefore, only slow flow speeds, or low sample concentrations, can be employed to avoid multiple molecular occupancies. Second, the larger the channel the greater noise contributions become from background interferences. By reducing channel dimensions to the nanometer scale, all analyte molecules can be maneuvered through a defined detection region and can be analyzed rapidly and with high signal-to-noise ratios.

In recent years, the creation of nanochannels or nanopores in thin membranes has attracted much interest due to the potential to isolate and sense single DNA molecules while they translocate through the highly confined channels.[5] Short translocation lengths make decontamination of the nanopores facile while maintaining effective spatial confinement for single-molecule detection. Nanopores for such applications have already been fabricated in insulating lipids,[6] silicon dioxide,[7] and silicon nitride[8,9] membranes and thus in principle may be integrated into monolithic analysis systems. In all studies to date, the detection of translocation events is performed electrically by measuring the ionic current.[10] In simple terms, molecules translocating through a nanopore will momentarily perturb the ionic current, with the duration of the perturbation and the magnitude of the current blockade providing more detailed information about molecular shape and structure. In the current letter, we present proof-of-concept studies that describe a novel approach for optically detecting DNA translocation events through an array of solid-state nanopores which allows for ultrahigh-throughput, parallel detection at the single-molecule level. Specifically, we optically probe fluorescently labeled DNA molecules translocating through sub-wavelength diameter pores within a thin aluminum/silicon nitride membrane. The opaque aluminum layer acts as an optical barrier between the illuminated region and the analyte reservoir. In these conditions, high-contrast imaging of single-molecule events can be performed.

The basic protocol used for manufacturing of our nanoporous membrane is shown in Figure 1. Briefly, a freestanding 200 nm thick silicon nitride membrane is fabricated
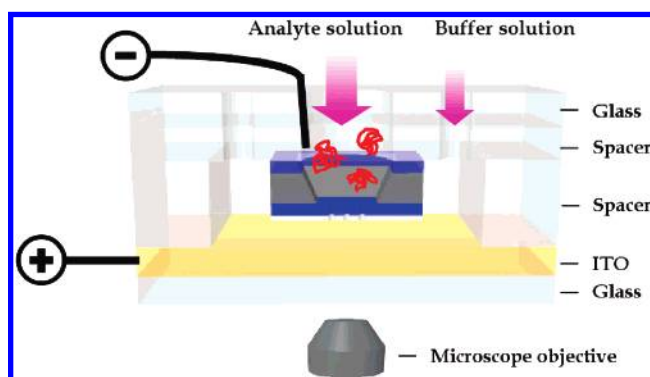
Figure 2. Schematic of experimental setup used to monitor DNA translocation events. Excitation light from a microscope objective is blocked by the membrane with the fluorescence signal from a translocating molecule collected by the same objective and directed to the emCCD camera. The cover slip is coated with a conductive layer of ITO. Solid-state nanopores have an average diameter of 300 nm.

using standard photolithographic techniques and KOH wet etching as previously described by Kim et al.[11] The membrane is then coated with a 100 nm thick aluminum layer by thermal evaporation. Subsequently, submicrometer-sized holes are milled in a sequential fashion using a focused ion beam (FIB) at 30 kV and 20 pA. Nanofluidic channels with a diameter between 250 and 300 nm are obtained after an exposure of 1−2 s at a magnification of 18−20 k×. Figure 1c shows typical results after milling nine 300 nm wide pores in the membrane. Such pores have an aspect ratio close to unity.

Double-stranded λ-DNA (48 kbp in length) duplexes were labeled with YOYO-1 (Molecular Probes) at a ratio of five base pairs per dye molecule and the solution diluted to yield a concentration of 10 pM. The membrane was mounted on a glass substrate (Figure 2) to form a sealed interface between the two reservoirs. Accordingly, the top reservoir is used to contain the analyte solution, with the lower reservoir containing buffer (50 mM phosphate, 200 mM KCl, pH = 7.4). Translocation of DNA through pores was initiated electrokinetically by applying a voltage between the upper and lower reservoirs. Assuming there is no potential drop at the interface between the electrodes and the solution, the effective electric field E across the pores would be equal to V/l, where V is the applied voltage and l the channel length (300 nm). For instance, a voltage of 200 mV corresponds to a field on the order of 6.7×10^5 V·m^{-1}. A glass cover slip
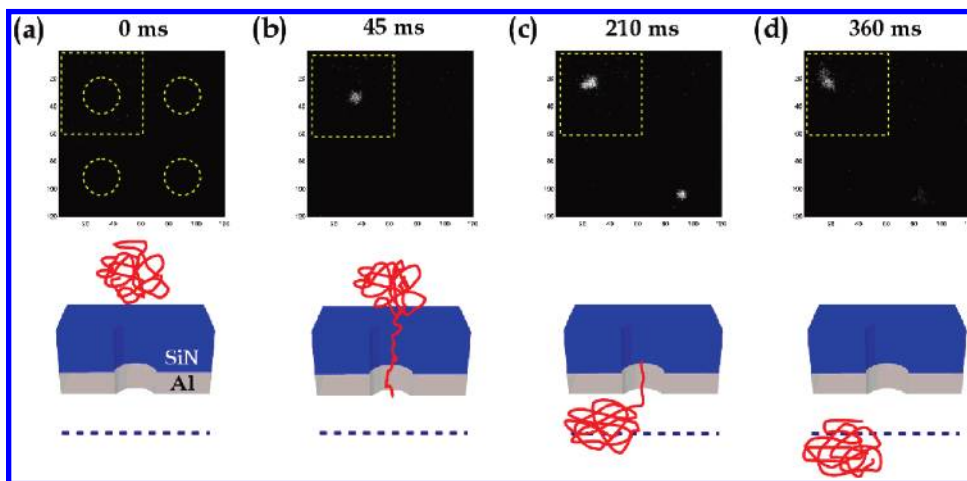
Figure 3. Fluorescence image of two DNA translocation events occurring under an applied voltage of 0.45 V at $t = 0$ (a), $t = 45$ ms (b), $t = 210$ ms (c), and $t = 360$ ms (d). Each pixel represents an area of 81×81 nm^2. The dotted circles in frame (a) indicate the location of the pores. Illustrations below each image frame provide an indication of the progression of DNA through the pore and the illumination plane (dotted line).

coated with a thin 100 nm film of indium tin oxide (ITO) is used to define the lower electrode, as shown in Figure 2. The distance between the aluminum pores and the ITO layer was set to be 30 μm by using a thin spacer, ensuring complete isolation. ITO was used in the current experiments as it is optically transparent and allows production of a uniform electric field at the bottom of the lower reservoir. The latter feature is crucial in allowing DNA to be transported quickly away from the detection probe volume subsequent to detection. Prior to addition of the buffer solution, the nanopore substrate is treated with an oxygen plasma to ensure the pore surfaces are hydrophilic in nature. Additionally, the plasma serves to grow a thin oxide layer on the aluminum that inhibits native aluminum dissolution under basic conditions.

Detection of DNA was achieved using a custom-built confocal microscope with imaging capabilities.[12] Briefly, the excitation light from a mercury lamp (filtered for 488 nm excitation) is focused onto the aluminum membrane surface using a high numerical aperture objective (60×). Because silicon nitride is optically transparent in the visible region of the electromagnetic spectrum, the aluminum layer is used to block any excitation light from illuminating the top reservoir, thus eliminating background cross-talk between the upper and lower reservoirs. This feature is important in removing all residual fluorescence associated with the top reservoir and hence maximizing the signal-to-noise ratio associated with translocation events. Fluorescence originating from translocating DNA molecules is then collected by the same objective and directed to an electron multiplying CCD (emCCD) camera (Cascade II, Photometrics). The camera has a pixel size of 16 μm, however, when used in conjunction with the 60× objective and a further 3.3× post-objective magnification, this generates an effective pixel size of 81 nm. This is significantly below the diffraction limit, resulting in translocation events being registered on an array of pixels with a fluorescence signature that is Gaussian in nature.

A variant of this setup was used to serially probe one pore at a time and provide superior time resolution to CCD imaging (microsecond versus millisecond resolution). In this configuration, an excitation laser beam is focused onto an individual pore and the fluorescence signal is acquired using an avalanche photodiode detector (AQR-141, EG&G, Perkin-Elmer). Details of this setup are provided in Supporting Information.

Translocation events of DNA molecules through the array of pores can be observed on a millisecond time scale. Figure 3 shows a sequence of images of typical translocation events for four pores under an applied voltage of 0.45 V (1.5 × 10^6 V·m^{-1}) as captured by the CCD camera. It should be noted that, although the CCD consists of 512×512 pixels, the area was cropped to a more defined region of interest of 200×200 pixels. This enables simultaneous probing of nine pores at a frame rate of approximately ∼15 ms (67 Hz). Figure 3b illustrates the onset of a translocation event in the top left hand pore. DNA passage through the field of view is complete after approximately 360 ms. Interestingly, the duration of the event is approximately 2 orders of magnitude greater than what has been reported by Smeets et al. using ionic current as a detection mechanism within a 10 nm wide and 60 nm thick pore.[13] In the experiment described, the membrane thickness of 300 nm results in a greater entropic effect to initiate complete translocation. Perhaps more importantly, as we are using an optical technique, fluorescence is continuously being detected from the onset of translocation until the DNA strand has completed translocation and departed from the field of view of the focal plane via a combination of electrokinetic and diffusive methods. This entire process is significantly longer in duration than measuring a blockage current. When the DNA is in the pore, fluorescence is isolated to the Al/pore interface; as the DNA strand translocates through the pore, the fluorescence signature is broadened and detected over a larger pixel range on the CCD. Once the translocation is completed, the molecule is no longer confined and can move from the axis of the pore (Figure 3c). By diffusing freely in the illuminated reservoir, the molecule gradually works its way outside of the focal plane, resulting in a progressive decrease in

fluorescence intensity (Figure 3d). A simultaneous translocation event is also observed on the bottom right pore.

The high contrast between the background and translocation events is directly attributable to the opaque properties of the aluminum layer. A thicker aluminum layer would in principle result in higher contrast; however, there is a compromise between the total length of the pore (in this case 300 nm) and the potential for pore blockage. Having said this, at a low applied voltage, this configuration allows discrimination of the successive translocation events while maintaining an acquisition area that is large enough for monitoring an array of 3 × 3 pores with 5 μm spacing between them. Higher-density arrays are clearly possible, and the pore spacing can be decreased down to 1 μm while maintaining sufficient optical resolution to resolve independent translocation events without cross-talk between the pores. Once translocation is complete, the DNA strand is driven toward the lower electrode, resulting in no increased background fluorescence. It should also be emphasized that, at the onset of experiments, the lower reservoir contains simply buffer. As the experiment progresses, the overall DNA concentration in the lower reservoir gradually increases, resulting in the possibility for a concomitant increase of the fluorescence background. This was not observed in our experiments as the whole reservoir is under illumination, and as a result, molecules are readily photobleached while being illuminated outside of the detection window.

The ionic strength of the buffer solution plays a crucial role in determining the threshold voltage at which the translocation occurs. Early experiments were carried out with a buffer solution containing 50 mM phosphate without the addition of monovalent electrolytes. For these experiments, the voltage needed to accomplish DNA translocation was in excess of 2 V, which induced sufficient Joule heating to create microscopic bubbles in the solution. Addition of 200 mM of KCl allowed for operation at sufficiently low voltages to negate this effect. At low salt concentrations (<100 mM), the effect of the negatively charged walls sets in, resulting in translocations being affected by the counterions that screen the walls.[14]

It is also found that the translocation behavior of the DNA molecules within the channels greatly depends on the hydrophilic state of the surface. On injection of the DNA solution immediately after oxygen plasma treatment, DNA molecules can diffuse freely through pores without the application of voltage. Although λ-DNA molecules are larger than the diameter of the pores (with a radius of gyration between 700 and 850 nm), the concentration gradient across the pores is sufficient to induce free translocations. Because the current oxygen plasma treatment has only a transitional effect, pores lose their hydrophilic character after a few hours. Accordingly, to ensure that the membrane did not allow any translocation without the application of a drive voltage, pores were wetted immediately after treatment and left for 4 h before injection of the DNA solution.

By recording a sequence of images and analyzing the intensities from the center of the pores using custom written Matlab algorithms, it is possible to monitor each pore as a
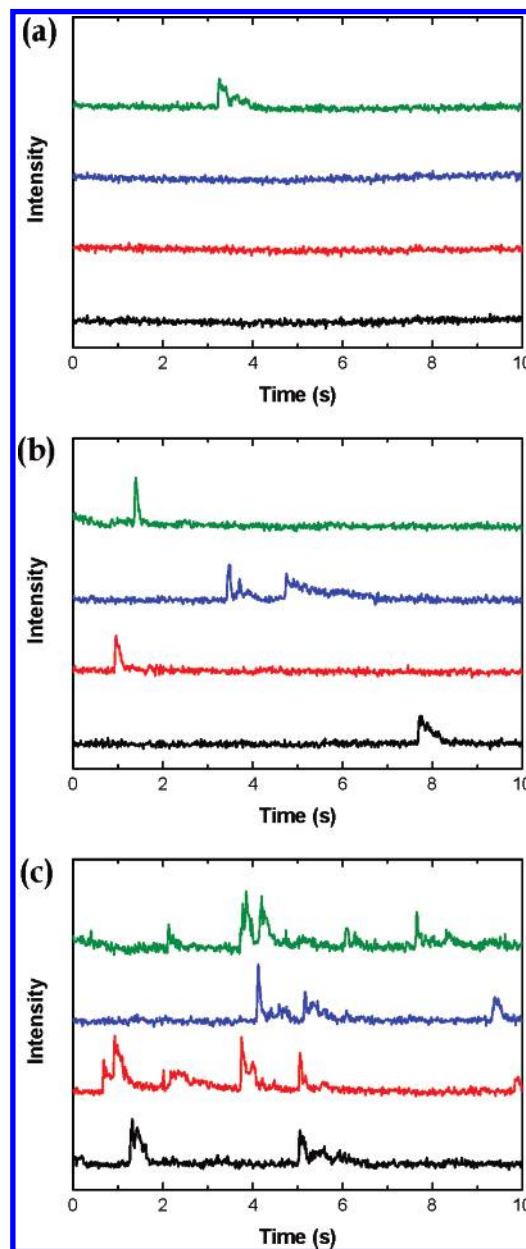
Figure 4. Variation of detected fluorescence as a function of time from four different pores under an applied voltage of 0.20 V (a), 0.30 V (b), 0.40 V (c). The vertical axis is arbitrary, and the four signals have been shifted vertically for convenience. All data were measured simultaneously.

function of time. Figure 4 illustrates the intensity values from four pores at different applied potentials. Observable peaks in each plot indicate simultaneous detection of translocation events through multiple pores. It is apparent that a higher voltage induces more translocation events to occur per unit time. Optical translocation events occur on a time scale between 100 and 800 ms depending on the applied voltage. For example, at an applied potential of 200 mV, a single translocation (taking 500 ms) was observed for four pores over a period of 10 s. Increasing the applied potential by 100 mV results in the observation of six events over the same time period and pore window. A further increase by 100 mV results in 25 translocations being registered. These experiments demonstrate successfully that a thin aluminum mem-
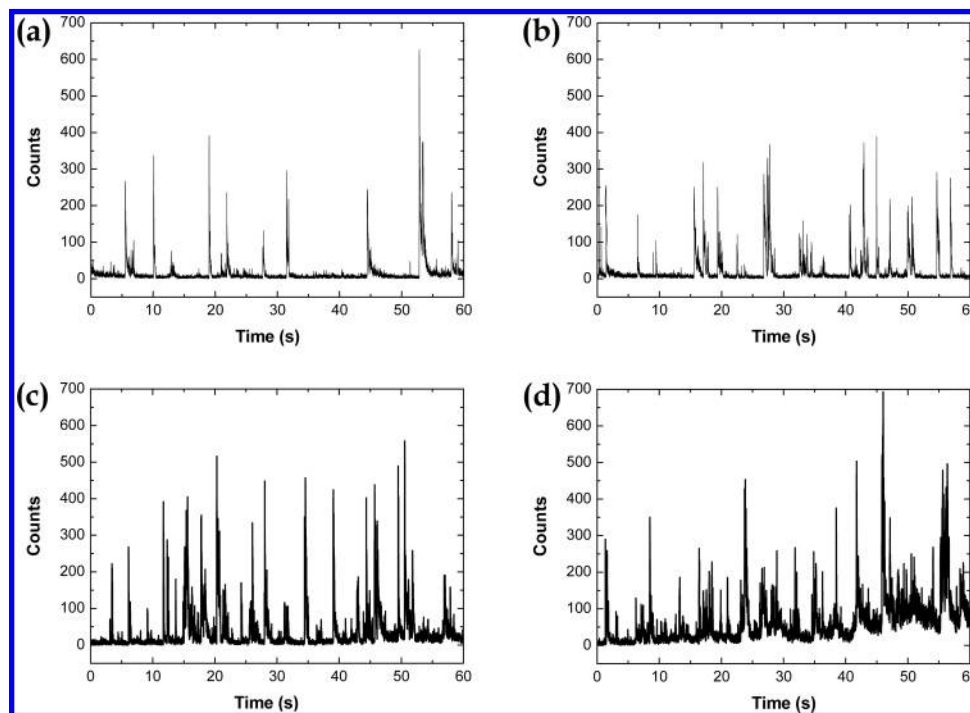
Figure 5. Fluorescence signal from a single pore acquired using an avalanche photodiode detector under applied voltages of 1.50 V (a), 1.60 V (b), 1.70 V (c), 1.90 V (d). Each peak corresponds to a single translocation event.

brane containing nanometer-sized holes can be used for parallel array detection (and ultimately high-throughput analysis) while maintaining the benefits of single-molecule resolution and high levels of molecular confinement. For example, in a conventional solution-based single-molecule detection experiment, approximately 10^3-10^4 molecules are detected within a 60 s time frame (1 molecule every 6–60 ms).[15] Using our synthetic nanopores, this value increases proportionally with the number of pores being analyzed simultaneously. By modifying the current chip configuration and optical components, we expect to be able to detect up to 10^2 pores simultaneously; this results in a 100-fold improvement in throughput while ensuring all analyte molecules pass through the detection probe volume. Importantly, it should be stressed that all fluorescent molecules that translocate are detected (100% detection efficiency), meaning that these devices will prove useful in applications such as rare event detection and diagnostics.

To further characterize translocation events, a single pore was probed using confocal optics (this results in a diffraction-limited Gaussian spot at the aluminum/pore interface). Although this approach reduces the overall throughput, there is a significant advantage in terms of time resolution and signal-to-noise ratio, enabling more efficient characterization of translocation events at higher potentials. Consequently, a separate experiment was performed with the same membrane but using an APD to probe the exit of a single pore under different applied voltages. Data were acquired at a time resolution of 50 μs and then resampled at 5 ms for plotting. The results are summarized in Figure 5 and are in excellent agreement with the translocation times measured using the emCCD. For a potential of 1.5 V, 14 peaks registered above the background threshold as defined by Poisson counting

statistics. Increasing the potential to 1.7 V resulted in 33 peaks over the same 60 s acquisition time. Increasing the voltage further resulted in a drastic increase in the overall baseline, implying that the rate of DNA translocation is sufficiently high that single-molecule events could no longer be resolved. Burst width and areas were determined to be on average 600 ms and 5900 photons, respectively, for an applied potential of 1.6 V. Increasing the potential resulted in not only shorter translocation times but also fewer registered photon counts attributed to the shorter residence times within the pore.

These proof-of-concept studies demonstrate for the first time optical detection of DNA translocation events through an array of solid-state nanopores. Results indicate that it is possible to obtain high spatial resolution DNA analysis while independently controlling the applied voltage that drives the molecules into the nanopore. A critical feature of the generic approach is the possibility of parallelizing molecular analysis by probing an entire array of nanopores under uniform illumination. Operations such as fragment sizing of DNA molecules are potentially achievable on time scales significantly shorter than with single-pore devices. We expect this work to have a high impact on the biomedical community and to open new routes to faster, parallel biomolecular analysis at the single-molecule level.

Supporting Information Available: Detailed description of the optical instrumentation used to serially prove individual nanopores. This material is available free of charge via the Internet at http://pubs.acs.org.

References

(1) deMello, A. J. *Nature* **2006**, *442*, 394−402.
(2) Dittrich, P. S.; Tachikawa, K.; Manz, A. *Anal. Chem.* **2006**, *78*, 3887−3908.
(3) Yan, X.; Grace, W. K.; Yoshida, T. M.; Habbersett, R. C.; Velappan, N.; Jett, J. H.; Keller, R. A.; Marrone, B. L. *Anal. Chem.* **1999**, *71*, 5470−5480.
(4) Eijkel, J. C. T.; van den Berg, A.; Manz, A. *Electrophoresis* **2004**, *25*, 243−252.
(5) Akeson, M.; Branton, D.; Kasianowicz, J. J.; Brandin, E.; Deamer, D. W. *Biophys. J.* **1999**, *77*, 3227−3233.
(6) Meller, A.; Nivon, L.; Brandin, E.; Golovchenko, J. A.; Branton, D. *Proc. Natl. Acad. Sci. U.S.A.* **2000**, *97*, 1079−1084.
(7) Storm, A. J.; Chen, J. H.; Zandbergen, H. W.; Dekker, C. *Phys. Rev. E* **2005**, *71*, 051903.
(8) Li, J.; Stein, D.; McMullan, C.; Branton, D.; Aziz, M. J.; Golovchenko, J. A. *Nature* **2001**, *412*, 166−169.
(9) Striemer, C. C.; Gaborski, T. R.; McGrath, J. L.; Fauchet, P. M. *Nature* **2007**, *445*, 749−753.
(10) Li, J. L.; Gershow, M.; Stein, D.; Brandin, E.; Golovchenko, J. A. *Nat. Mater.* **2003**, *2*, 611−615.
(11) Kim, M. J.; McNally, B.; Murata, K.; Meller, A. *Nanotechnology* **2007**, *18*, 205302.
(12) Huebner, A.; Srisa-Art, M.; Holt, D.; Abell, C.; Hollfelder, F.; deMello, A. J.; Edel, J. B. *Chem. Commun.* **2007**, *12*, 1218−1220.
(13) Smeets, R. M. M.; Keyser, U. G.; Krapf, D.; Wu, M. Y.; Dekker, N. H.; Dekker, C. *Nano Lett.* **2006**, *6,* 89−95.
(14) Dekker, C. *Nat. Nanotechnol.* **2007**, *2*, 209−215.
(15) Stavis, S. M.; Edel, J. B.; Li, Y. G.; Samiee, K. T.; Luo, D.; Craighead, H. G. *Nanotechnology* **2005**, *16*, S314−S323.

NL071855D